Journal of Neuropathology and Experimental Neurology

Vol. 57, No. 1
January, 1998
pp. 76–94

N-terminal Heterogeneity of Parenchymal and Cerebrovascular Aβ Deposits

TINA L. TEKIRIAN, BA, TAKAOMI C. SAIDO, PHD, WILLIAM R. MARKESBERY, MD, MICHAEL J. RUSSELL, PHD, DAVID R. WEKSTEIN, PHD, ELA PATEL, AND JAMES W. GEDDES, PHD

Abstract. The goals of this study were twofold: to determine whether species differences in Aβ N-terminal heterogeneity explain the absence of neuritic plaques in the aged dog and aged bear in contrast to the human; and to compare Aβ N-terminal isoforms in parenchymal vs cerebrovascular Aβ (CVA) deposits in each of the species, and in individuals with Alzheimer disease (AD) vs nondemented individuals. N-terminal heterogeneity can affect the aggregation, toxicity, and stability of Aβ. The human, polar bear, and dog brain share an identical Aβ amino acid sequence. Tissues were immunostained using affinity-purified polyclonal antibodies specific for the L-aspartate residue of Aβ at position one (AβN1[D]), D-aspartate at N1 (AβN1[rD]), and pyroglutamate at N3 (AβN3[pE]) and p3, a peptide beginning with leucine at N17 (AβN17[L]). The results demonstrate that each Aβ N-terminal isoform can be present in diffuse plaques and CVA deposits in AD brain, nondemented human, and the examined aged animal models. Though each Aβ N-terminal isoform was present in diffuse plaques, the average amyloid burden of each isoform was highest in AD vs polar bear and dog (beagle) brain. Moreover, the ratio of AβN3(pE) (an isoform that is resistant to degradation by most aminopeptidases) vs AβN17(L)-x (the potentially nonamyloidogenic p3 fragment) was greatest in the human brain when compared with aged dog or polar bear. Neuritic plaques in AD brain typically immunostained with antibodies against AβN1(D) and AβN3(pE), but not AβN17(L) or AβN1(rD). Neuritic deposits in nondemented individuals with atherosclerotic and vascular hypertensive changes could be identified with AβN1(D), AβN3(pE), and AβN1(rD). The presence of AβN1(rD) in neuritic plaques in nondemented individuals with atherosclerosis or hypertension, but not in AD, suggests a different evolution of the plaques in the two conditions. AβN1(rD) was usually absent in human CVA, except in AD cases with atherosclerotic and vascular hypertensive changes. Together, the results demonstrate that diffuse plaques, neuritic plaques, and CVA deposits are each associated with distinct profiles of Aβ N-terminal isoforms.

Key Words: Alzheimer disease; Canine; Human; Polar bear.

INTRODUCTION

In the aged human brain, β-amyloid (Aβ) is associated with senile plaques and with cerebrovascular angiopathy. The human brain exhibits at least 3 types of senile plaques: classical plaques with neurites and amyloid cores, primitive plaques with neurites and no amyloid cores, and diffuse plaques without neurites or amyloid cores (1). Within gray matter, diffuse, amorphous-type plaques can exist in the absence of mature, neuritic plaque deposits (2). Diffuse Aβ deposits are often considered nontoxic, nonfibrillar, soluble deposits (characterized by both random-coil and alpha-helical structure), while aggregated Aβ (cored) plaques are more insoluble and are considered neurotoxic (3–8).

Diffuse plaques can be present in both nondemented individuals and in those with AD, whereas neuritic deposits are associated with AD. Aβ deposits have also been found in the brains of aged dogs, cats, bears, and nonhuman primates (9–13). The 42-amino acid Aβ sequence of the dog and polar bear is identical to that of monkey and human (14). In aged dogs, Aβ is present in diffuse plaques without neuritic or neurofibrillary pathology as defined by silver stains and tau immunostaining (15–17). The aged polar bear brain has diffuse plaques and neurofibrillary tangles, but not neuritic plaques (17). Diffuse and neuritic plaques can also be found in some aged primates (18–21).

The distribution of Aβ deposits in the human brain and in the aged animal models appears similar. For example, a row of plaques is often observed in the outer molecular layer of the dentate gyrus in AD and in nondemented elderly brains (17, 22, 23). In the outer molecular layer of the dentate gyrus, aged beagles demonstrate diffuse hippocampal clouds of Aβx-42, while these Aβ plaques are more distinct in the polar bear (17). A similar distribution of Aβ has been observed in transgenic mice, which overexpress a mutant amyloid precursor protein (PDAPP V717F) and develop advanced AD pathology (24).

In addition to full-length Aβ1-42, there are several amino- and carboxyl-terminal truncated Aβ isoforms. Aβ, a 4kD peptide, is produced by proteolytic cleavage of the β-amyloid precursor protein (APP) by an unidentified β-secretase (N-terminus clip) and γ-secretase(s) (C-terminus clips) (Fig. 1; for review see [25]). The C-terminus may be modified further by additional proteases, resulting in the generation of Aβx-40 and Aβx-42. A 3kD peptide (p3) that originates at Aβ amino acid 17(L) can

From the Sanders-Brown Center on Aging, Alzheimer's Disease Research Center and Department of Anatomy and Neurobiology (TLT, WRM, DRW, EP, JWG), Pathology & Neurology, University of Kentucky, Lexington, KY 40536; the Department of Molecular Biology (TCS), Tokyo Metropolitan Institute of Medical Science, Bunkyo-ku, Tokyo 113, Japan; and the Department of Anesthesiology (MJR), University of California, Davis, CA 95616.

Correspondence to: Dr James W. Geddes, Sanders-Brown Building, Room 209, 800 S. Limestone Street, University of Kentucky, Lexington, KY 40536-0230.

Contributions of each author: TLT: experiments, analysis, and manuscript preparation; TCS: dot blot analysis, production and characterization of the antibodies; WRM: neuropathologic evaluation; MJR: characterization of canine tissue; DRW: procurement of polar bear tissue; EP: experiments; JWG: experiments, analysis, manuscript preparation.

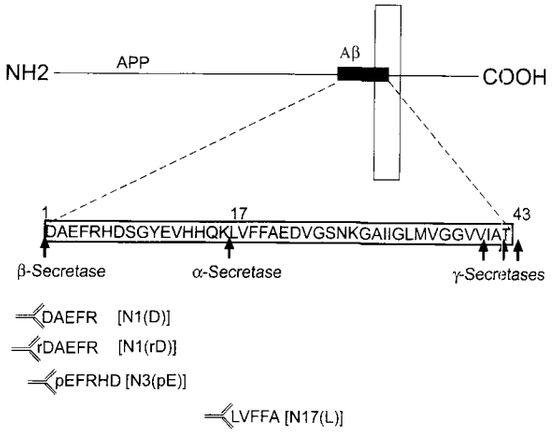

Fig. 1. N-terminal heterogeneity of β-amyloid. β-amyloid (Aβ) is generated from the β-amyloid precursor protein (APP) by putative β- and γ-secretases that cleave (respectively) at the amino and carboxyl termini of Aβ. The amino terminus can be further modified by racemization (conversion of D to rD) or by proteolysis followed by conversion of the glutamate at position 3 to a pyroglutamate residue. APP can also be cleaved by α- and γ-secretases, producing a shorter 3kD peptide (p3) that begins at position 17(L) of Aβ. Antibodies used to distinguish between these Aβ isoforms were produced using synthetic peptides DAEFRC (AβN1[D]); rDAEFRC (AβN1[rD]); and pEFRHC (AβN3[pE]). The antibody against p3 (N17[L]) was raised against an Aβ17-40 peptide and affinity-purified to collect antibodies that specifically recognized p3 and eliminated regions which may cross-react with full-length Aβ. Production and characterization of the antibodies is described by Saido and colleagues (34, 50).

be formed by the combined actions of α-secretase and γ-secretase. Biochemical studies have revealed additional N-terminal Aβ isoforms. The first amino acid of the 4kD Aβ peptide is L-aspartate (AβN1[D]), which can be isomerized (AβN1[iD]) or racemized (AβN1[rD]) (26). Aβ can also begin at position 3 with a glutamate, which may be converted to pyroglutamate (AβN3[pE]) (27). The cyclization of a glutaminyl residue into a pyroglutamyl residue is a common step in post-translational processing of biologically active peptides such as neurotensin and leuteinizing hormone–releasing hormone (28). Amino- and carboxyl-terminal truncated Aβ isoforms differ in terms of aggregation and toxicity (29–35). In vitro, truncation at the C-terminal diminishes Aβ aggregation and toxicity (e.g. Aβ1-40 vs 1-42) (4). In contrast, isoforms truncated at the N-terminus [Aβ8-42 and Aβ17-42 (p3)] aggregate more readily and are more toxic than Aβ1-42 (33).

Previous investigations have examined the temporal and spatial localization of Aβ C- and N-terminal isoforms in the human brain. At the C-terminus, a series of studies have shown that Aβx-42 is prevalent in diffuse plaques, while Aβx-40 is present in a subset of neuritic (cored) plaques (32, 36, 37). At the N-terminus, Saido and colleagues (34) have observed that AβN3(pE) is more abundant, and may be deposited earlier than AβN1(D). In a subsequent study, this group indicated that the major deposited N-terminal isoforms include AβN1(rD), AβN3(pE), or AβN11(pE), and that p3 is a minor constituent of senile plaques (38). These investigators neither distinguished between isoforms associated with control (nondemented) vs AD cases nor identified specific constituents of neuritic vs diffuse plaques. Furthermore, AβN1(rD), AβN3(pE), or AβN11(pE) distribution in cerebrovascular amyloid (CVA) has not been examined in AD brain. Cordell and colleagues (39) observed that the p3 is present in diffuse plaques and in some dystrophic neurites, but not in plaque cores or CVA. Wisniewski and colleagues (40) have documented that though p3 is prevalent in Down syndrome cerebellar diffuse plaques, this isoform is a minor component of neuritic plaques due to oxidation. This study also indicated an absence of Aβ17-42 in a leptomeningeal amyloid preparation, while a separate investigation by Wisneiwski and colleagues (15) revealed p3 immunoreactivity in the cerebral vessels and diffuse plaques of aged dogs. In addition, p3 appears to exhibit topographic specificity as it is more prevalent in cerebellar diffuse plaques as compared with deposits in the cerebral cortex and is sparse or absent in the striatum (41). Lemere et al (42) have observed AβN1- and AβN3(pE)- immunoreactive cerebral vessels in Down Syndrome brain, but did not examine p3 or AβN1(rD) in these tissues. Lastly, Russo and coworkers (43) have indicated that the concentration of AβN3(pE), a dominant species of soluble Aβ in AD and Down syndrome (DS) brains, increases with age in DS and serves as the earliest marker of Aβ aggregation.

The reason why neuritic plaques develop in the aged human and aged primates, but not in other aged mammals, is unknown. Younkin (44) suggests that Aβx-42 deposition initiates the development of AD pathology. However, Aβx-42 is present in diffuse plaque and cerebrovascular β-amyloid deposits in the aged dog (beagle) and polar bear, yet these animals do not develop neuritic plaques (17). P3 may confer protection against neuritic plaque formation (40) and has been proposed as specific to AD pathology (39). Cyclization of AβN3(E) into AβN3(pE) has also recently been hypothesized as specific to AD brain and is believed to play a critical role in the pathogenesis of this neurodegenerative disorder (43).

The first goal of the present study was to determine if species differences in Aβ N-terminal heterogeneity might help to explain the absence of neuritic plaques in the aged dog and aged bear in contrast to the human. The second goal was to compare Aβ N-terminal isoforms in parenchymal vs cerebrovascular Aβ deposits in each of the species and in individuals with Alzheimer disease vs nondemented subjects.

TABLE 1
Cases Examined (Human, Polar Bear, and Canine)

Case	Species	Age	Sex	Diagnosis	Cause of death/other conditions
1	Human	79	F	AD (15 years)	
2	Human	74	M	AD (12 years)	Bronchopneumonia
3	Human	82	M	AD (8 years)	Hypertension
4	Human	85	M	AD (15 years)	Bronchopneumonia
5	Human	71	F	AD (10 years)	
6	Human	67	M	AD (5 years)	Ischemic/hypoxic injury (hippocampus)
7	Human	81	F	AD (3 years)	Bronchopneumonia
8	Human	83	M	AD (4 years)	
9	Human	73	F	AD (10 years)	
10	Human	58	F	AD (7 years)	Pulmonary emboli
11	Human	87	M	AD (20 years)	Cerebral atherosclerosis
1	Human	81	F	CONTROL	Acute pneumonia
2	Human	88	M	CONTROL	Multifocal atherosclerosis (anterior & posterior vascular tree)
3	Human	87	M	CONTROL	Chronic obstructive pulmonary disease
4	Human	89	F	CONTROL	Pneumonia, acute myelocytic leukemia, hypertension
5	Human	80	F	CONTROL	Cerebral atherosclerosis, hypertension
1	Polar bear	25–29	F		Euthanized, advanced age
2	Polar bear	35	M		Euthanized, lame, back injury
3	Polar bear	35	F		Natural advanced age
4	Polar bear	30	F		Natural advanced age
5	Polar bear	36	F		Euthanized, renal disease, liver complications
6	Polar bear	NA			Cause of death unknown
7	Polar bear	20	F		Hepatic cancer
8	Polar bear	36	F		Euthanized, disoriented, ataxic
9	Polar bear	13	F		Multifocal myocitis-diaphragm
1	Canine	14.2	M		
2	Canine	16.6	M		
3	Canine	16.6	F		
4	Canine	15	F		
5	Canine	14.1	F		
6	Canine	13.3	M		
7	Canine	14.5	F		
8	Canine	17.4	M		
9	Canine	14.9	M		
10	Canine	16.6	F		

MATERIALS AND METHODS

Sixteen human brains, taken from individuals ranging in age between 58–89, were provided by the University of Kentucky Alzheimer's Disease Research Center (ADRC) brain repository (Table 1). Eleven of these patients (6 male, 5 female) had histories of progressive dementia and met NINCDS-ADRDA clinical criteria for the diagnosis of AD (45); all patients met accepted neuropathological criteria for the diagnosis of AD (46, 47). Five control subjects were individuals without a history of dementia, and who lacked other neurologic disorders and systemic disorders affecting the brain. These cases were participants in a normal volunteer control group who have annual neuropsychological testing; all had test scores within the normal range. At autopsy, these individuals demonstrated minimal AD pathology.

The nine polar bears, aged 13–36, examined in this study were obtained from 5 different zoos (Denver, Colo; Knoxville, Tenn; Royal Oak, Mich; Tacoma, Wash; and Toledo, Ohio). The aged beagle tissues (Table 1) were obtained from the National Radiobiology Archives, as described previously (17).

Immunohistochemistry

At autopsy, all brain specimens (human, polar bear, and canine) were immersion fixed in 10% neutral-buffered formalin; fixation time ranged between 3 days and 3 weeks. After fixation, the tissues were paraffin-embedded in an identical manner. Blocks containing the hippocampal formation, parahippocampal gyrus, temporal cortex, and inferior temporal gyrus were sectioned at 10 μm. All tissue sections were deparaffinized through graded alcohols and xylenes, pretreated with 90% formic acid (3 min) (48), pepsin (10 min) (49), and 3% H_2O_2 in methanol (30 min). Sections were blocked in 15% horse serum, then incubated with primary antibody overnight at room temperature. Primary antibodies included affinity-purified polyclonal anti-N1(D) (1:1000 dilution), anti-N3(pE) (1:1000 dilution), anti-N1(rD) (1:500 dilution), and anti-N17(L) (1:100 dilution). Antibody dilutions were optimized in order to minimize background staining. The production and characterization of the antibodies has been described previously (34, 50). Standard Tris-buffered saline (TBS) (145 mmol/L NaCl, 50 mmol/L Tris,

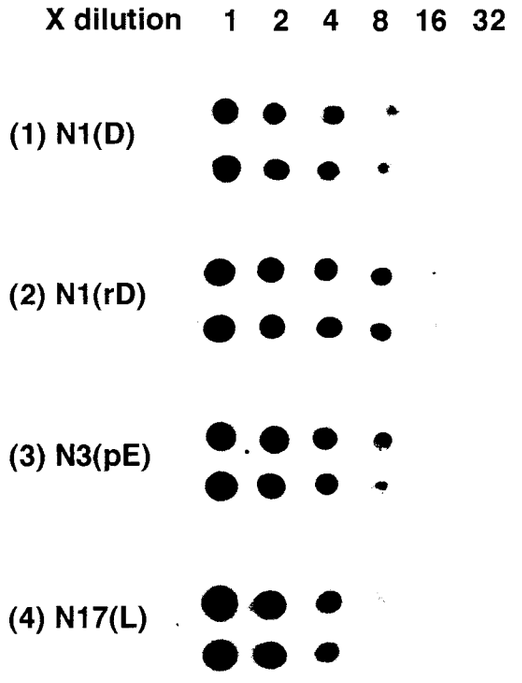

Fig. 2. Specificity of the anti-Aβ N-terminus antibodies. The specificity of each Aβ antibody was examined by dot blot analysis (see Materials and Methods). Serial dilutions of the corresponding pentapeptide (2-fold serial dilution of 10μg/ml in distilled water) were reacted with each of the antibodies. The results illustrate similar specificities of each of the peptides against the corresponding antigen.

dH_20, pH 7.4) was used in order to rinse the tissue after pretreatments, primary, and secondary antibody steps. Following incubation with primary antibody, sections were treated with a goat-anti-rabbit IgG biotinylated secondary antibody (Vector Laboratories, Burlingame, Calif) followed by avidin-biotin complex (AβC Elite Kit, Vector). Color visualization was attained with 3,3′ diaminobenzidine (Sigma) or metal-enhanced diaminobenzidene (Pierce, Rockford, IL). Negative controls for immunolabeling included omission of the primary antibody and substitution of the primary antibody with normal serum. All sections were examined and photographed with an Olympus BH-2 or an Olympus Provis AX70 microscope.

Modified Bielschowsky Staining

Modified Bielschowsky staining was executed according to the method of Yamamoto & Hirano (51). Averaged neuritic plaque counts were based upon the mean of ten areas counted in each hippocampus and temporal cortex while tangle counts were based upon the mean of 5 areas counted in each of these regions. Neuritic plaques and neurofibrillary tangles were counted per 2.35 mm^2 (Table 4).

In pilot studies, the following fixation conditions were compared with 10% neutral-buffered formalin sections: 4% paraformaldehyde followed by antigen retrieval citrate buffer (BioGenex, San Ramon, Calif) and microwaving for 15 minutes, and 70% ethanol fixation. Results obtained with formalin and formic acid pretreatment were similar to 4% paraformaldehyde tissues exposed to antigen retrieval. Previous studies also indicate that formic acid does not negatively affect the detection of the examined isoforms (34, 50). Both of these conditions revealed more deposits than the 70% ethanol fixation. The ethanol-fixed sections could not be dipped in formic acid or microwaved, as these treatments destroyed the tissue.

Congo Red Staining

8-μm sections were dried at 40°C in an oven overnight. Slides were deparaffinized in xylene and hydrated through graded alcohols to double distilled water. The slides were stained with Weigert's Hematoxylin (1.0 g hematoxylin crystals, 100 ml 95% alcohol, 4 ml ferric chloride [29% aqueous], 95 ml distilled water, and 1 ml hydrochloric acid) for 8 seconds (microwaved), washed in running distilled water for 30 seconds, differentiated in acid alcohol for 30 seconds, rinsed in water once again, stained in Congo Red solution (0.5 g Congo Red, 100 ml 50% ethyl alcohol) for 30 seconds, then rinsed in distilled water for 8 minutes. Next, the slides were dehydrated in a series of alcohols (70→100%) (two minutes each dip), cleared in xylene, and mounted with Permount™. Sections were visualized by polarized light examination (52) using apple green fluorescence with a dark background as an indication of tinctorial-positive deposits. Diffuse deposits are not Congo-red positive in contrast to amyloid deposits, which are Thioflavin S– and Congo-red stained (53, 54).

Thioflavin Staining

8-μm sections were mounted on uncoated slides, incubated 40°C overnight, deparaffinized through xylenes and alcohols, rinsed in distilled water, and placed in Thioflavin S solution (0.5 g Thioflavin S (Polysciences, Warrington, Pa) in 50 ml distilled water for 2 minutes. The slides were differentiated 3 times in 80% ethanol, washed in water, then coverslipped with VectaShield (Vector, Burlingame, Calif) mounting medium.

Image Analysis

For image analysis of the percent area occupied by the various N-terminal isoforms, images were captured on a Mayo Biosciences Image Analysis System, consisting of a workstation (Digital Equipment Corporation Alpha Station 250 4/266), Quantim software, a Pulnix color CCD camera, and an Olympus Vanox Microscope. The dimensions of each microscopic field (working display image frame size) measured 525μm (maximum x-axis) × 396μm (maximum y-axis). Images were acquired using a 10× objective. The percent area occupied by Aβ deposits was determined by automatic thresholding, based on both intensity and color fractionation (such methodology has been documented in a previous study [55]). Areas that lacked cerebrovascular Aβ deposits were assessed in the image analyses; hence, the data represent quantitation of strictly parenchymal plaques. For each antibody (AβN3[pE], AβN1[D], AβN1[rD] and AβN17[L]), 3 to 4 fields in 2 separate cortical regions were evaluated. All cases were imaged within the same session, maintaining constant illumination parameters.

TABLE 2
Semi-Quantitative Scoring of Aβ N-Terminal Isoform Abundance in Parenchymal Plaques

	AβN3(pE)	AβN1(D)	AβN1(rD)	Aβ17(L)
AD				
1	DP +++ CP ++	DP +++ CP ++	DP +	DP ++
2	DP +++ CP +++	DP ++ CP ++	DP +	DP ++
3	DP +++ CP ++	DP +	DP +	DP +
4	DP +++ CP +	DP ++ CP +	DP ++	DP ++
5	DP ++ CP ++	DP +	DP +	DP +
6	DP ++ CP ++	DP + CP +	DP +	DP +
7	DP ++ CP +	DP ++ CP +	DP +	DP +
8	DP +++ CP +	DP ++ CP +	DP ++	DP +
9	DP + CP +	DP ++	DP +	DP ++
10	DP ++ CP +	DP +++	DP +	DP ++
11	DP ++ CP +	DP +	DP +	DP +
Human control				
1	0	0	0	0
2	DP ++ CP +	DP ++ CP +	DP + CP +	DP +
3	DP +	DP +	0	0
4	DP ++ CP +	DP ++ CP +	DP + CP +	DP + CP +
5	DP ++ CP +	DP ++ CP +	DP + CP +	DP +
Polar bears				
1	DP +	DP +	DP +	DP +
2	0	DP +	DP +	DP +
3	0	DP +	DP +	DP +
4	DP +	DP +	DP +	DP +
5	0	DP +	DP +	DP +
6	0	0	0	0
7	DP +	DP +	DP +	DP +
8	DP +	DP +	DP +	DP +
9	0	0	0	0
Canine				
1	DP +	DP +	0	DP +
2	DP +	0	0	DP
3	DP +	DP +	0	DP +
4	DP +	DP +	0	0
5	DP +	DP +	0	0
6	0	0	0	0
7	DP +	DP +	0	DP +
8	DP +	DP +	DP +	DP +
9	0	0	0	0
10	0	0	0	0

Dot Blot Analysis

2 μl of synthetic Aβ peptide solution (2-fold serial dilution of 10 μg/ml in distilled water) was spotted on a PVDF (polyvinylidene difluoride) membrane and dried at 60°C for 20 min. After brief (1 to 2 seconds) soaking in methanol, the membrane was blocked in 20 mM Tris/HCL (pH 7.5) containing 500 mM NaCl, 0.1% Tween 20, and 10 mg/ml bovine serum albumin for 1 hour (h) at room temperature. The membrane was then incubated with the primary antibody (anti-Aβ antibodies) diluted (1μg/ml) in the Tris/HCL state above for 1 h. After washing, the immunoreactive signals were visualized employing an Fab fragment of donkey anti-rabbit IgG antibody conjugated to peroxidase and visualized using enhanced chemiluminescence (ECL) (Amersham). Each antibody used in this study was completely absorbed by the corresponding hapten peptide in dot blot and immunocytochemical analyses (not shown).

RESULTS

To determine that each antibody was specific for the corresponding peptides targeted in this study, dot blots containing serial dilutions of the antigenic peptides were reacted with each antibody (Fig. 2). The results illustrate similar specificities of each of the peptides against the corresponding antigen. The production and characterization of each antibody has been described previously (34, 50).

Alzheimer Disease

Neuritic plaque and neurofibrillary tangle (NFT) counts in the temporal cortex and hippocampus were obtained in order to assess the severity of pathology in each

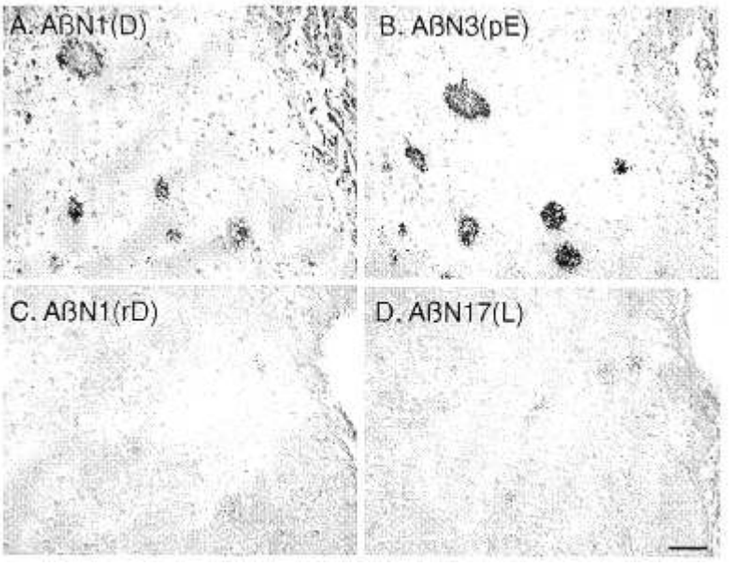

Fig. 3. In Alzheimer disease, diffuse plaques were labeled with each of the antibodies against Aβ N-terminal isoforms. In an individual with AD (age 85, M), fewer diffuse plaques were immunolabeled with AβN1(D) (A) than by AβN3(pE) (B). Immunostaining in adjacent sections with AβN1(rD) (C) and AβN17(L)(D) demonstrated fewer deposits and less robust staining than that observed with AβN1(D) and AβN3(pE). Scale bar = 50μM.

case (Table 4). Consistent with previous studies that indicate that the presence of abundant cortical NFT corresponds with dementia (for example, [56]), NFT were rare in the cortex of control cases but abundant in AD cases examined in this study.

Diffuse deposits were characterized by a faint, cloud-like, amorphous appearance, whereas mature (cored) deposits were distinct and strongly immunostained. Some cored deposits were surrounded by a diffuse halo. As the anti-Aβ N-terminus antibodies alone do not reveal plaque neurites, modified Bielschowsky stain was used to specifically identify neuritic plaques on corresponding sections.

Each of the 11 AD cases (Tables 1, 2) examined had numerous diffuse and neuritic (cored) plaques. Although each human AD case had diffuse deposits which labeled with each antibody, not all plaques in each of the cases labeled with all 4 Aβ N-terminal antibodies. In the temporal cortex, anti-AβN3(pE) revealed the most diffuse deposits, followed by antibodies against AβN1(D), AβN17(L), and finally AβN1(rD), which labeled the fewest deposits. Similar results were obtained in the dentate gyrus molecular layer, a region that lacks cored deposits. Antibodies anti-AβN3(pE) and AβN1(D) immunostained diffuse deposits more robustly than anti-AβN17(L) and anti-AβN1(rD) (Fig. 3).

A distinct pattern of immunostaining was observed in the cored, neuritic plaques. Cored plaques were labeled by anti-AβN3(pE) in each of the 11 AD cases, by AβN1(D) in 6 of the 11 cases, and were not labeled by AβN1(rD) or Aβ17-x in any of the AD cases. Neither age nor disease duration could explain the differences in the immunostaining of cored plaques in the examined AD patients.

Nine of the 11 AD cases were also characterized by cerebrovascular Aβ deposits (Table 3). Three of these AD cases demonstrated evidence of cerebrovascular complications (vascular hypertensive changes, hypoxia-ischemia, and cerebral atherosclerosis). In these cases, Aβ deposits in both cortical and leptomeningeal vessels were intensely immunoreactive with all 4 antibodies (Figs. 5, 6). The remaining 6 individuals revealed mild to moderate CVA. Of these cases, one displayed minor reactivity with all 4 antibodies, and 3 had leptomeningeal vascular deposits that reacted with 3 of the antibodies (AβN3[pE], AβN1[D], and AβN17[L]). In 2 cases, CVA in leptomeningeal vessels was immunostained with antibodies against N1(D) and AβN17(L). The pattern of the Aβ N-terminal isoforms in the cortical vessels typically paralleled that observed in leptomeningeal vessels (Table 3).

Nondemented Elderly

Three individuals (Tables 1, 2) had diffuse plaques that immunostained with each Aβ N-terminus antibody. None of the nondemented elderly controls exhibited dentate gyrus outer molecular layer amyloid pathology. In one individual, diffuse plaques were labeled with only 2 of the antibodies, AβN3(pE) and AβN1(D). In one case, Aβ deposits were not detected with any of the antibodies. Three of the control cases were characterized by cerebral atherosclerosis and/or vascular hypertensive changes (Table 1). In each of these individuals, neuritic plaques were

TABLE 3
Semi-Quantitative Scoring Of Aβ N-Terminal Isoform Abundance in Cerebrovascular Amyloid

	AβN3(pE)	AβN1(D)	AβN1(rD)	Aβ17(L)
AD				
1	LM +	LM + CV+	0	LM + CV +
2	0	0	0	0
3	LM +++	LM +++	LM +++	LM +++
	CV +++	CV +++	CV +++	CV +++
4	LM +	LM + CV+	0	LM + CV +
5	LM +	LM + CV+	0	LM + CV +
6	LM +++	LM +++	LM +++	LM ++
	CV +++	CV +++	CV +++	CV ++
7	0	LM + CV+	0	LM + CV+
8	0	LM + CV+	0	LM + CV+
9	LM + CV +	LM + CV+	LM + CV +	LM + CV +
10	0	0	0	0
11	LM +++	LM +++	LM +++	LM +++
	CV ++	CV +++	CV +++	CV ++
Human control				
1	LM +	LM ++	LM 0	LM +
		CV +++	CV ++	
2	0	0	0	0
3	0	0	0	0
4	LM + CV+	LM + CV +	LM + CV+	LM + CV+
5	LM +	LM +	0	LM +
Polar bears				
1	0	0	0	0
2	0	0	0	0
3	LM + CV+	LM + CV +	LM +	0
4	0	0	0	0
5	0	0	0	0
6	0	0	0	0
7	LM + CV+	LM + CV+	0	LM + CV +
8	LM + CV+	LM + CV+	LM + CV +	LM + CV +
9	0	0	0	0
Canine				
1	LM + CV +	LM + CV +	LM +	LM + CV +
2	LM + CV +	LM + CV +	LM +	LM + CV +
3	LM + CV +	LM + CV +	LM +	LM + CV +
4	LM + CV +	LM + CV +	LM +	LM + CV +
5	0	0	0	0
6	0	0	0	0
7	LM + CV +	LM + CV +	LM + CV +	LM + CV +
8	LM + CV +	LM + CV +	0	LM + CV +
9	LM + CV +	LM + CV +	0	LM + CV +
10	LM + CV +	LM + CV +	0	LM + CV +

present and immunostained with antibodies against AβN3(pE), AβN1(D), and AβN1(rD). In one of these 3 individuals, a few cored deposits were also labeled with anti-AβN17(L) (Fig. 4). This individual was the only subject, of the 16 human cases examined, in which anti-AβN17(L) immunostained cored deposits. In addition, this particular individual (age 89, F) was the oldest individual examined in this study.

Three of the nondemented control cases demonstrated leptomeningeal cerebrovascular Aβ (CVA) deposits (Table 3). In one individual, leptomeningeal and cortical CVA were mildly immunoreactive with each of the 4 antibodies; leptomeningeal cerebrovascular deposits in another case were labeled with 3 of the N-terminus antibodies (AβN1[D], AβN3[pE] and AβN17[L]), while one individual had leptomeningeal vascular deposits stained with the same 3 antibodies, but lacked cortical vascular Aβ deposits.

Polar Bears

Seven of the 9 polar bears had diffuse Aβ deposits in the temporal cortex that immunostained with each N-terminal antibody (Fig. 7) (Table 2). While the antibody against AβN1(rD) labeled diffuse plaques in each of the

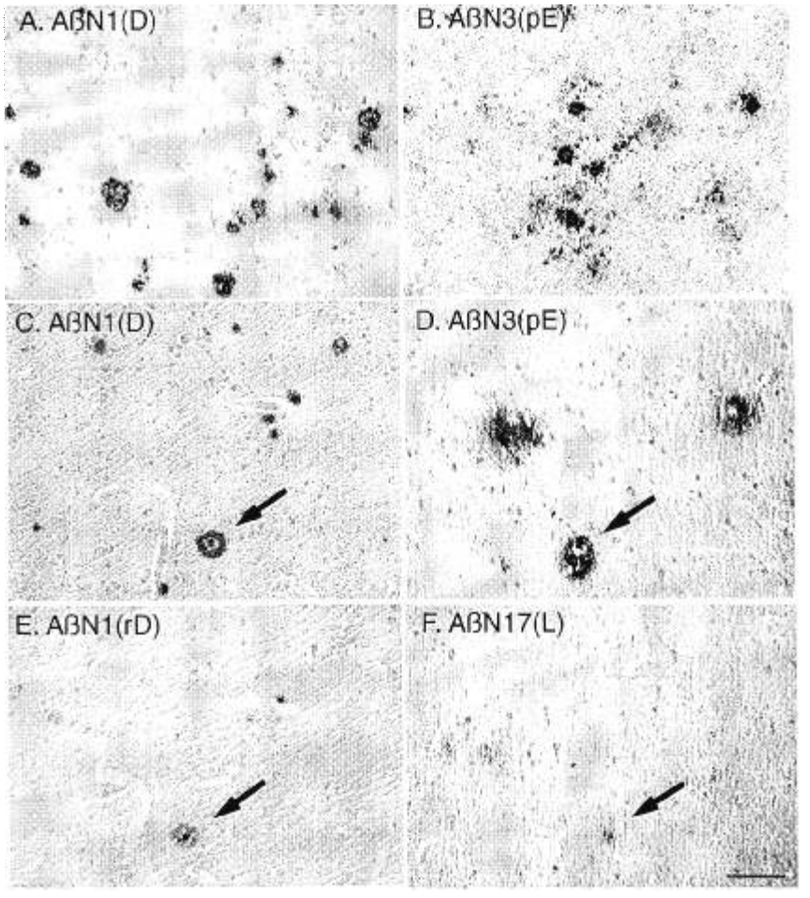

Fig. 4. Classical (cored, neuritic) plaques were evident in AD cases as well as nondemented elderly with cerebrovascular disorders. In an individual with AD (74, M), AβN1(D) (A) and AβN3(pE) (B) immunostained many cored deposits that were not recognized by anti-AβN17(L) or anti-AβN1(rD) (not shown). In a nondemented individual with a clinical history of hypertension (89, F), AβN1(D) (C) recognized a cored deposit, also recognized by AβN3(pE) (D), AβN1(rD) (E), and AβN17(L) (F). Arrows indicate a cored deposit which was immunostained by antibodies in panels C–F. Scale Bar = 50 μM.

polar bears, the staining was faint and plaques were not as numerous as those stained with the other antibodies. Only 2 of the polar bears had plaques in the dentate gyrus outer molecular layer. These plaques were stained with 3 antibodies in 1 polar bear (AβN3[pE], AβN1[D], and AβN17[L]), and 2 antibodies (AβN3[pE] and AβN1[D]) in the second animal.

Three polar bears had leptomeningeal CVA deposits (Table 3). In one animal, cortical and leptomeningeal vascular Aβ deposits were immunostained with each N-terminus antibody, although AβN1(rD) was sparse. In another bear, cortical vascular and leptomeningeal deposits were labeled with AβN1(D), AβN3(pE), and AβN17(L), but lacked AβN1(rD) antibody immunostaining. The remaining polar bear exhibited leptomeningeal vascular deposits that were labeled with AβN1(D), AβN1(rD), and AβN3(pE), but not AβN17(L). The only polar bears without deposits were the youngest one examined in this study and another animal whose age was undetermined by the zoo of origin. Neither polar bear nor beagle brain contained neuritic plaques, as assessed by Bielschowsky staining.

Canine

Seven of the 10 beagles had diffuse plaques (Table 2). The plaques were less strongly stained (Fig. 7) than those in the human or polar bear. There was marked individual variation in the pattern of Aβ N-terminus staining observed. One dog had diffuse plaques that immunostained with each N-terminus antibody. Three beagles had deposits labeled with 3 antibodies (AβN1[D], AβN17[L], and AβN3[pE]). AβN1(D)- and N3(pE)-immunopositive diffuse plaques were revealed in 2 beagles. A single dog had diffuse deposits that labeled with anti-AβN3(pE) and anti-AβN17(L). Overall, 6 of the 7 canine cases lacked AβN1(rD) in diffuse plaques. In 2 dogs, AβN1(D) and AβN3(pE) immunostained a broad diffuse band in the dentate gyrus outer molecular layer (DGOML).

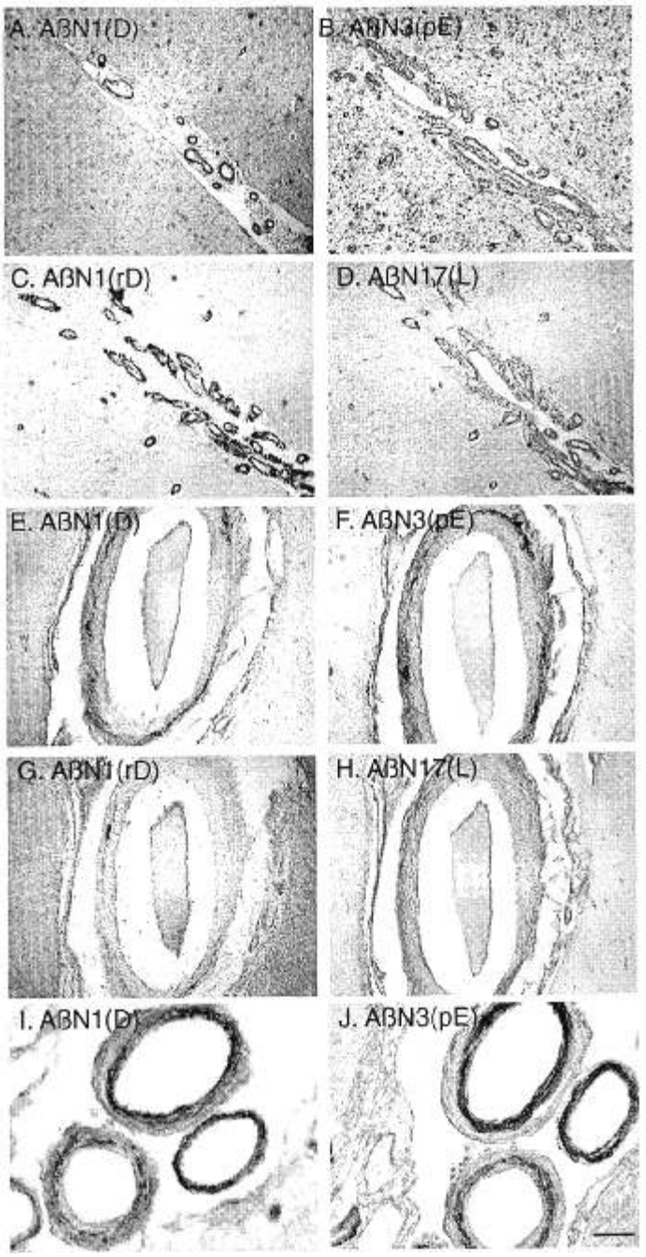

Fig. 5. Leptomeningeal blood vessels immunolabeled with each N-terminus antibody in AD cases with marked cerebrovascular deposition. An individual with AD (82, M) (A–D) demonstrated leptomeningeal blood vessels that immunostained with all of the N-terminal isoforms examined. These include AβN1(D) (A); AβN3(pE) (B); N1(rD) (C); and N17(L) (D). Scale bar (A–D) = 10 μM. In a polar bear (36, female), leptomeningeal vascular Aβ deposits were labeled with antibodies against AβN1(D) (E) and AβN3(pE) (F). AβN1(rD) recognized a lesser amount of amyloid (G), while AβN17(L) immunostaining of leptomeninges was absent in this case (H). In a beagle (16.6, male), leptomeningeal vascular Aβ immunostained with antibodies against AβN1(D) (I) and AβN3(pE) (J). Scale Bar = 50 μM.

In contrast to the relatively weak Aβ immunostaining in canine diffuse plaques, leptomeningeal and cortical CVA deposits in the dogs were robustly stained (Fig. 5). Eight of the 10 dogs exhibited cerebrovascular amyloid (Table 3). The 4 N-terminal antibodies labeled leptomeningeal Aβ in 5 dogs, and 3 antibodies (AβN3[pE], AβN1[D] and AβN17[L]) stained the leptomeningeal CVA in 3 dogs. Similar results were observed in cortical vascular Aβ deposits, which were detected by the same 3 antibodies in 7 cases, and in all 4 antibodies in the remaining 1 dog. Cerebrovascular amyloid deposits could be stained with both Thioflavin S or Congo-Red (Fig. 6), while diffuse plaques in the dogs and polar bears were not observed with these stains.

Image Analysis

To quantify the observations, image analysis was used to determine the relative load of each N-terminus Aβ isoform (Table 5) (Fig. 10). In the aged human brain, the vast majority of cases had a greater load (burden) of AβN3(pE) as compared with AβN1(D) (Fig. 8). The mean AβN3(pE) burden in AD brain was 6.0% ± 1.0 (standard error of the mean [SEM]) in contrast to a mean of 3.8 % ± 0.6 in control, nondemented brain (Table 5). This result is similar to that observed by Saido and colleagues (34) in a study that assessed the number of plaques that labeled with each antibody (plaques were counted; however, plaques in AD vs control brain were not compared). The relative load of AβN1(D) was greater than AβN17(L) in most individuals, and greater than AβN1(rD) in all cases examined. The mean AβN1(D) burden in AD brain was 3.0 % ± 0.6, while AβN1(D) burden in control brain was only 1.6 % ± 0.2. AβN1(rD) burden in AD brain was 1.0 % ± 0.4 in contrast with 0.4% ± 0.2 in nondemented individuals, while AβN17(L) in AD brain revealed a burden of 1.8 % ± 0.4 vs 0.3% ± 0.1 in controls (Table 5). Comparison of AβN17(L) vs AβN1(rD) revealed an equivalent or greater load of AβN17(L) in all but one of the cases examined. Similar results for each comparison were observed with plaques in the dentate gyrus molecular layer, except that the relative load of AβN1(rD) was only 0.1% ± 0.1 (mean ± s.e.m.), much less than in temporal cortex where the percent area occupied by AβN1(rD) was 1.0% ± 0.4.

Many of the aged nonhuman mammals had a similar number of plaques immunostained with AβN1(D) and AβN3(pE) (Fig. 8). However, 3 polar bears exhibited a greater ratio of AβN3(pE)/AβN1(D), and 4 dogs had measurable levels of AβN3(pE), but not AβN1(D). Similar to the human brain, most brains of other mammals had a greater abundance of AβN1(D) than AβN17(L). All but one of the nonhuman mammal brains had greater loads of AβN1(D) than AβN1(rD). In most of the aged nonhuman mammals, AβN17(L) was more abundant than

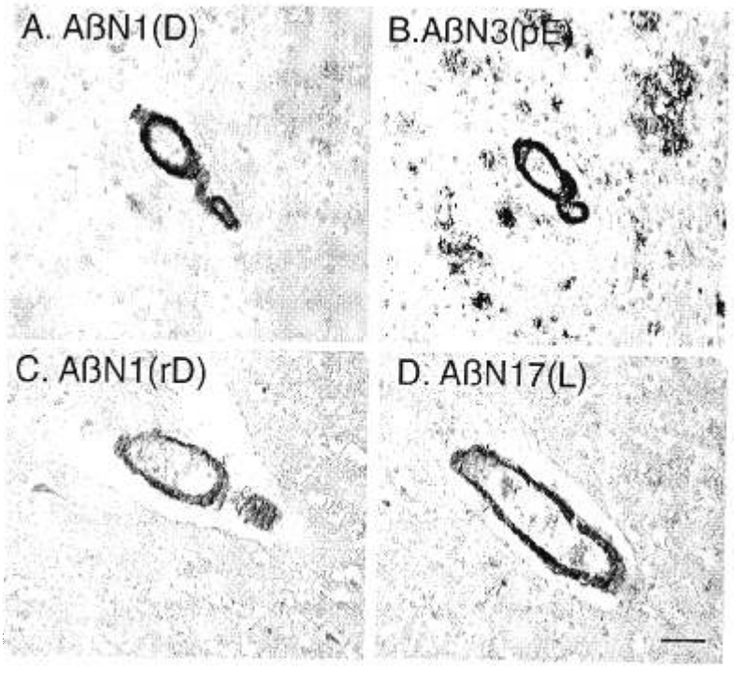

Fig. 6. Parenchymal, cortical vessels were immunolabeled by each N-terminus antibody in AD cases with marked cerebrovascular amyloid deposition. An 82-year-old male with AD and a history of hypertension displayed cortical vessels containing Aβ (serial sections) that were recognized by AβN1(D) (A), AβN3(pE) (B), AβN1(rD) (C), and AβN17(L) (D). Scale Bar = 50 μM.

AβN1(rD). The relative load of the various Aβ N-terminal isoforms was similar in aged polar bears and nondemented elderly human individuals.

DISCUSSION

Aβ N-terminal Isoforms in Plaques

Each of the evaluated Aβ N-terminal isoforms (AβN1[D], AβN1[rD], AβN3[pE], and AβN17[L] or [p3]) was present in diffuse plaques in each of the examined species. These results demonstrate that neither AβN17(L)-x nor AβN3(pE)-x are specific to AD brain, in contrast to previous suggestions (39, 43). Though the 4 examined Aβ N-terminal isoforms could be present in diffuse plaques of each species, the absolute loads for each isoform were greatest in individuals with AD. A critical mass of Aβ may be necessary for its aggregation into more compact deposits associated with neuritic plaques. In vitro, Aβ solubility and aggregation into β-sheet oligomers is influenced by peptide concentration and incubation time (57). In vivo, diffuse plaques are formed prior to neuritic plaques in Alzheimer disease (58). The development of diffuse and neuritic plaques is thought to be accelerated in Down syndrome due to a gene dosage effect (these individuals carry 3 copies of chromosome 21, the locus of the amyloid precursor protein) (59). In addition, transgenic mice which overexpress a mutant form of APP have been shown to develop diffuse plaques prior to the appearance of more highly aggregated deposits (24, 60, 61). The shorter lifespans of the aged dog and polar bear, as compared to humans, may account for their minor accumulation of extracellular Aβ and lack of neuritic plaques. However, neuritic plaques have been documented in aged primates of similar age to the polar bears in the present study (20).

If a critical mass of total extracellular Aβ is necessary for the development of neuritic plaques, the similar total abundances of Aβ N-terminal isoforms in the polar bear vs nondemented elderly individuals suggests that occasional neuritic plaques should be evident in the polar bear. The absence of neuritic plaques in the polar bear and presence of neuritic deposits in AD brain may reflect the abundance of specific Aβ N-terminal isoforms. AD brain contains higher levels of AβN3(pE) than nondemented human and polar bear brains, while polar bear brain contains relatively high levels of p3 [AβN17(L)-x] in comparison with human control brain.

Pyroglutamate-containing Aβ peptides are resistant to major aminopeptidases (34, 50, 62) and are hypothesized to play a critical role in the formation of neuritic deposits (43, 50). In contrast, p3 has been considered "nonamyloidogenic" (40, 63). In Down syndrome cerebellum (a region which precludes neuritic plaque development), p3 is present at relatively high levels in diffuse deposits. Although p3 may aggregate even more readily than Aβ1-42, p3-immunopositive deposits appear amorphous in

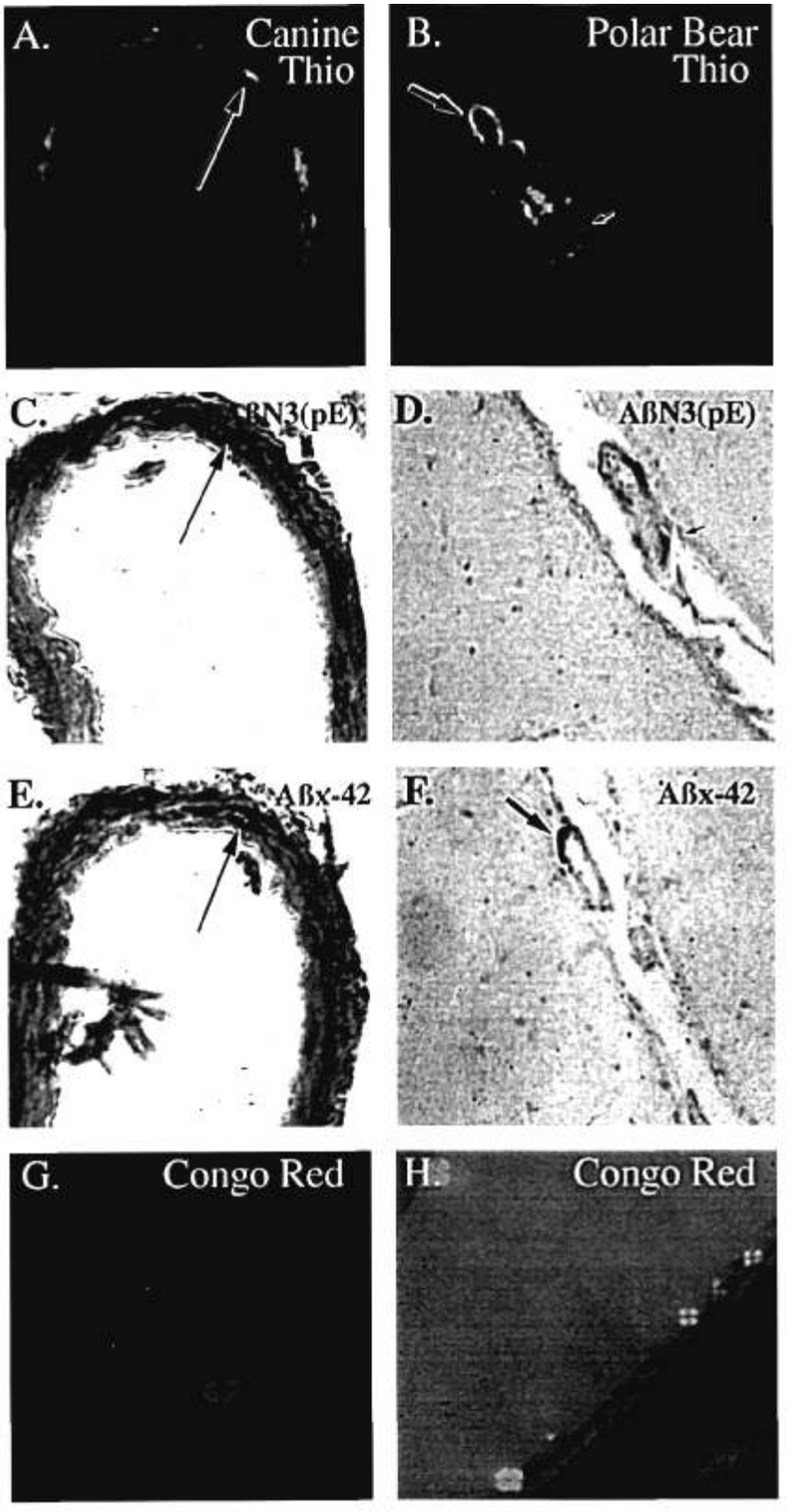

Fig. 7. Thioflavin S– and Congo red–positive cerebrovasculature in polar bear and dog. Thioflavin S revealed tunica media amyloid staining in the respective depicted vessels of a dog (14.5 years old, female) (A) and a polar bear (25–29 year old, female) (B). Tunica media staining was also observed in serial sections with anti-AβN3(pE) (canine[C], polar bear [D]) and anti-Aβx-42 (canine [E], polar bear [F]). Antibody characterization and dilution of x-42 is as described previously (17). Congo red staining in both the dog (G) and the polar bear (H) revealed a Maltese-cross–like pattern of staining. Arrows indicate shared localization of pathology in the canine (A, C, E) and polar bear cerebrovasculature (B, D, F). Scale Bar = 50 μM.

TABLE 4
Mean Values of Neurofibrillary Tangles and Neuritic Plaques in Hippocampus and Temporal Cortex

	Neuritic plaques		Neurofibrillary tangles	
Case	Hippocampus	Temporal cortex	Hippocampus	Temporal cortex
Alzheimer disease				
1	CA1 100	N/A	28	21
2	N/A	25	N/A	30
3	CA1 14.8	14.4	24.4	18.2
4	CA1 45	18.4	14.4	22.6
5	CA1 83	35.3	34	30.6
6	75	75	N/A	N/A
7	CA1 30.4	15.1	54.4	30.6
8	CA1 46.5	15.4	25	36.4
9	Dent gyr 50	75	N/A	N/A
10	N/A	100	49	25
11	Dent gyr 50	50	N/A	N/A
Human control				
1	0	0	0	0
2	CA1 0	17.5	3.6	1.0
3	CA1 0	0	4	0
4	20	4.5	9.4	0.4
5	CA1 26.9	12.8	3.0	0.8

Demented human (AD) cases exhibited abundant neocortical neurofibrillary tangles (NFT) in contrast to nondemented controls, which often lacked cortical tangles; this supports the view that NFT serve as a strong neuropathologic correlate of dementia (56). In both AD and control brain, neuritic plaques visualized by Bielschowsky stain were also identified with Aβ N-terminal antibodies (see Table 2). Bielschowsky-stained NFT and NP counts depict mean values in 10 microscopic fields in both the hippocampus and the temporal cortex (see Materials and Methods). All controls had Mini-Mental State Exam scores between 26 and 29 (maximum score = 30).

contrast to the fibrils formed by Aβ1-42 (33, 40). Moreover, p3 lacks the Aβ region critical for complement activation and recruitment of glia to plaques (64), and may thus play a protective role in diffuse plaques.

If all neuritic plaques arise from diffuse deposits, it would be expected that similar Aβ N-terminal isoforms would be present in both types of plaques. However, diffuse plaques contain all N-terminal isoforms examined, while AD cored deposits typically lack AβN17(L)-x (p3) and AβN1(rD). The presence of p3 in many diffuse deposits, but its absence in most neuritic plaques, suggests that certain neuritic plaques arise independently of diffuse deposits, that p3 may be lost from cored deposits, or that the detection of p3 is prevented in cored deposits through hindrance by more abundant isoforms. The presence of p3 cored deposits in only the oldest of the 16 cases examined in this study (89-year-old female) supports the suggestion of Iwatsubo and colleagues (38) that p3 may accumulate substantially at only late stages of plaque formation.

An inability to detect AβN1(rD)-x in cored deposits in the AD brain contrasts with a previous study which demonstrated racemized aspartate in isolated plaque cores (65). A possible explanation for the different results may be due to less racemization of aspartate at position one of the amino-terminus as compared with internal residues of Aβ. However, this phenomenon is unlikely, as N-terminal amino acids are expected to undergo more rapid racemization (66). Tomiyama and colleagues (67) have reported that racemization of Aβ depends upon the position of the amino acid in question. For instance, racemization of aspartate at position 23 accelerates Aβ1-35 peptide aggregation, while racemization at an aspartate in position 7 slows down this reaction; these colleagues did not examine a peptide with racemized aspartate at position 1.

Cored, neuritic deposits in nondemented individuals with hypertension and atherosclerosis were robustly immunostained with the antibody against AβN1(rD). These AβN1(rD)-immunopositive, cored deposits were in the same region as neuritic plaques (as determined using modified Bielschowsky stain) on corresponding sections from the same tissue blocks, and appeared similar to the morphology of neuritic plaques in AD cases. The finding

TABLE 5
Mean Aβ Load Values in Temporal Cortex

Isoform	AβN3(pE)	AβN1(D)	AβN17(L)	AβN1(rD)	AβN3(pE)/ AβN17(L)	TOTAL Aβ
AD	6.0 ± 1.0	3.0 ± 0.6	1.8 ± 0.4	1.0 ± 0.4	4.8 ± 0.8	11.8 ± 1.6
Control	3.8 ± 0.7	1.6 ± 0.2	0.3 ± 0.1	0.4 ± 0.2	8.5 ± 3.0	6.1 ± 0.9
Polar bear	2.1 ± 0.4	2.0 ± 0.5	1.4 ± 0.5	0.2 ± 0.1	1.5 ± 0.6	5.7 ± 0.8
Canine	0.8 ± 0.4	0.3 ± 0.5	0.2 ± 0.4	0.2 ± 0.1	2.6 ± 0.6	1.5 ± 1.1

The Aβ burden (mean ± SEM) for each N-terminal isoform examined in temporal cortex indicates that AD brain contains more of each isoform when compared with control human, polar bear, and canine brains. Human control and dog values of Aβ17(L) and AβN1(rD) resembled each other, while AβN3(pE) was at least twice as abundant as AβN1(D) in both AD and control brain. AβN3(pE) load was slightly higher than AβN1(D) in the canine, while similar AβN3(pE) and AβN1(D) values were exhibited in polar bear brain. The sum total of all Aβ N-terminal isoforms examined was highest in AD, similar in control human and polar bear brains, and lowest in the canine brain. Scatterplots that depict the individual amyloid load values of each Aβ N-terminal isoform are displayed in Figure 10.

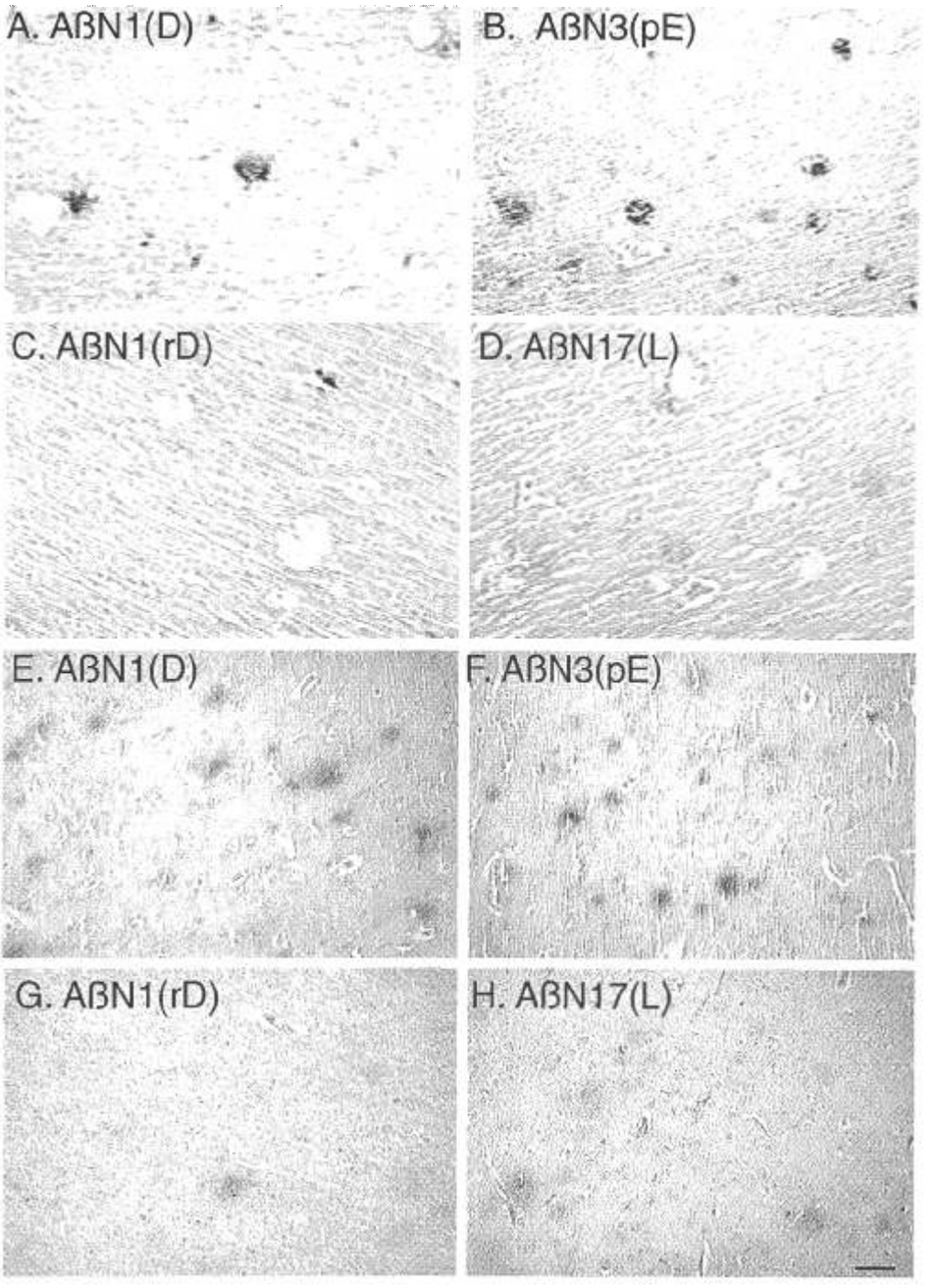

Fig. 8. Each N-terminus antibody revealed diffuse deposits in the canine (beagle) as well as the polar bear. In an 17.4-year-old beagle, AβN1(D) (A) labeled fewer deposits than AβN3(pE) (B). In adjacent sections, AβN1(D) and AβN3(pE)-immunopositive plaques barely immunostained with an antibody against AβN1(rD) (C), and labeled very faintly with anti-AβN17(L) (D). In a polar bear (35, female), a similar number of plaques were labeled by AβN1(D) (E) and AβN3(pE) (F). Many fewer deposits were faintly stained with antibodies against AβN1(rD) (G) or AβN17(L) (H). Scale Bar = 50 μM.

→

Fig. 9. Percentage area occupied by Aβ N-terminal antibodies as calculated via color discrimination–based image analysis. Plaques in the temporal cortex of an individual affected by Alzheimer disease (79, F) are shown in the top panel (A). The depicted

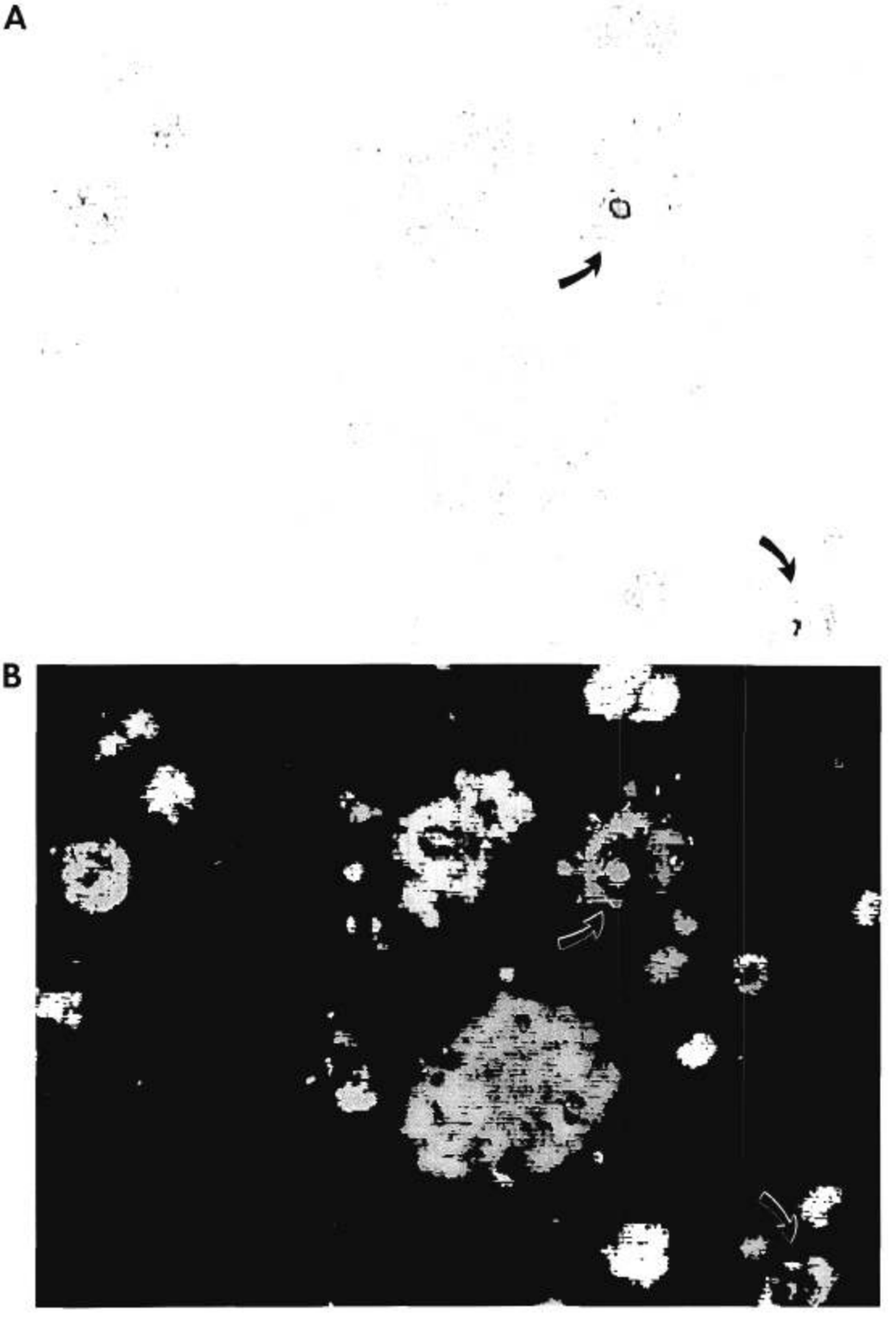

plaques (A) were captured, processed, and color thresholded by a Mayo Biosciences Image Analysis System consisting of a workstation, Quantim software, a Pulnix color CCD camera, and an Olympus Vanox Microscope; the resultant image is depicted in the bottom panel (B). Working display measurements are documented in the Materials and Methods section. The area of plaques in image B was calculated as 10.04%. Arrows indicate examples of the specificity of the image analysis method.

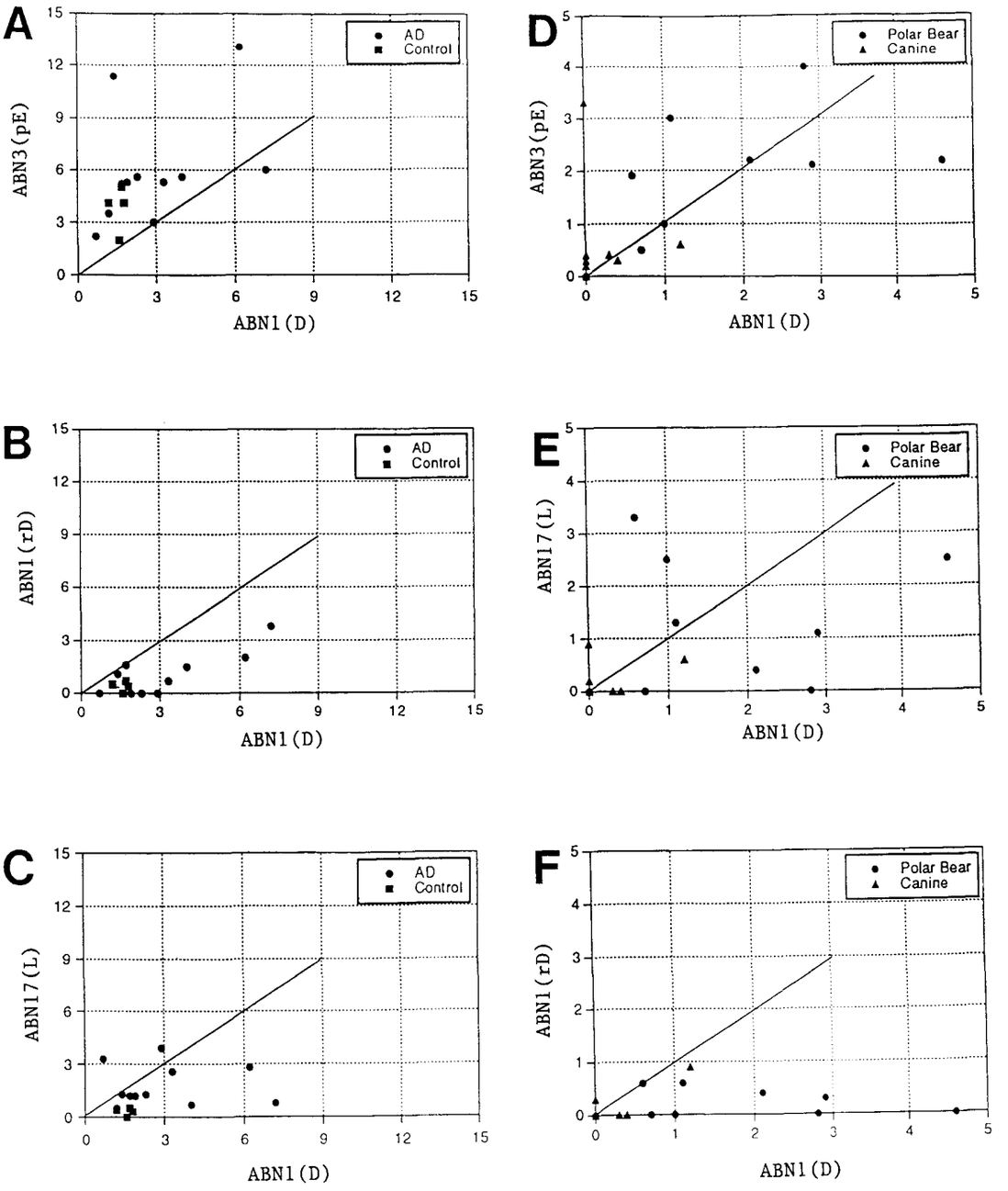

Fig. 10. Relative load of Aβ N-terminus isoforms in the temporal cortex. The relative load of AβN3(pE) was much greater than that of AβN1(D) in both nondemented elderly individuals and in those with AD (A). The load of AβN1(D) was typically greater than that of AβN1(rD) and AβN17(L) (B, C). In the polar bear, the relative abundance of AβN3(pE) was often similar to that of AβN1(D) (D), while AβN1(D) was similar in abundance to AβN17(L) (E) and more abundant than N1(rD) (F). In the canine brain, low loads of each Aβ N-terminus species were observed.

of AβN1(rD)-x cored deposits in non-AD controls, but not in AD cases, cannot be explained by technical issues, since tissue fixation, processing, and pre-treatments were similar in all cases. The presence of cored deposits in non-AD tissue is consistent with observations of classical plaques in nondemented individuals with significant cerebral atherosclerosis (68). Identification of AβN1(rD) in neuritic plaques in nondemented individuals with vascular hypertensive or atherosclerotic changes, but not in AD, suggests a different evolution of the plaques in the

2 conditions. Racemization of amino acids is generally very slow, suggesting that neuritic plaques in these nondemented individuals may have been present for a longer duration than the neuritic plaques observed in AD. However, Saido suggests that amino-terminal modifications, including racemization, occur prior to Aβ deposition (50). Along these lines, the results suggest accelerated racemization of Aβ in individuals with vascular disorders, possibly due to local conditions such as pH fluctuations associated with atherosclerosis.

N-terminal Aβ Isoforms in Cerebrovascular Deposits

Cortical leptomeningeal and cerebrovascular Aβ deposits could be immunostained by each of the four N-terminus antibodies in the aged human, dog, and polar bear brain, although there was considerable intersubject variability (see Results). Intense leptomeningeal and cortical arterial deposition of all 4 Aβ N-terminal isoforms was observed in 3 of the AD cases with cerebral atherosclerosis, hypertensive, and hypoxic changes. AβN1(rD)-x, which was not detected or sparse in the CVA of most other cases, was robustly present in these cases. This observation may reflect the greater abundance of cerebrovascular Aβ in the cases with vascular disorders, greater ages of the deposits, or local conditions such as pH. The detection of AβN17(L)-x in the cerebrovasculature of AD brain contrasts with the observations of Cordell and colleagues (39) who did not detect p3-positive CVA with a different anti-p3 antibody. However, p3 has been previously observed in canine CVA (15).

In most of the aged beagles, CVA was prevalent and was robustly immunostained with each of the N-terminus antibodies. This result contrasted with faint staining of diffuse plaques in the same animals. CVA was sparse in the aged polar bear and the immunostaining of these deposits was relatively weak. Our study is the first report of the examined isoforms (with the exception of p3) in the aged polar bear and beagle brain and indicates that the propensity for Aβ to be truncated and/or modified into such isoforms is not a human-specific quality.

Source of N-Terminal Isoforms

The relative abundance of N-terminus isoforms in Aβ deposits presumably reflects a steady-state of the processes of secretion, proteolysis, and additional intra- and extracellular modifications. Cultured cells can secrete AβN1-x, Aβ17-x, x-42, and x-40 (69, 70–74). 4kD Aβ is secreted in greater abundance than p3 in cultured human neurons and astrocytes (75). Whether AβN3(pE)-x is produced intracellularly and then secreted or is instead generated by extracellular proteolysis is unknown. Certain cell types have been linked to the secretion of Aβ N-terminal-truncated peptides. For instance, Madin-Darbin Canine Kidney (MDCK) cells expressing endogenous or

TABLE 6
Distribution of Aβ C- and N-Terminal Isoforms in AD, Nondemented Human, Aged Beagle and Polar Bear Brain

Aβ isoform	Aβx-42/43*	Aβx-40*	AβN1(D)	AβN1(rD)	AβN17(L)-x	AβN3(pE)
Diffuse plaques	All species	Absent	All species	Can be observed in all species though abundance is low in dog brain	All species	All species
Cored plaques	AD & aged nondemented	AD	AD & ND***	Strictly ND***	Typically absent**	Ad & ND***
Cerebrovascular Aβ	All species	All species	All species	This isoform was observed in the CVA of those affected by AD and atherosclerotic & vascular hypertensive changes. Can also be observed in polar bear and dog brains	All species	All species

* C-terminal data obtained from (17). ** AβN17(L)-x was observed in neuritic deposits of one human case in this study, the oldest individual examined (89-year-old female). *** Nondemented individuals with atherosclerotic and/or vascular hypertensive changes.

transfected amyloid β-precursor protein have been associated with oligomers enriched with amino-terminal–truncated Aβ species beginning at Arg 5 (76). Moreover, small amounts of SDS-stable Aβ oligomers enriched in Arg 5 have also been documented in the culture media of Chinese Hamster Ovary cells, which express endogenous or transfected APP (77). Furthermore, increased levels of alternatively cleaved N-terminal Aβ species are characteristic of cells which express an Ala→Gly mutation at position 692 of APP770 (78).

AβN1(rD) presumably arises from racemization of extracellular AβN1(D), although whether this conversion occurs intra- or extracellularly is also unexamined in vitro. Though truncated Aβ N-terminal modifications have been reported in vitro, the secreted amounts of such isoforms are low (77). Along these lines, it is logical to assume that a lengthy timespan is necessary in order to accumulate N-terminal–truncated isoforms in vivo.

In summary, this study demonstrates that Aβ N-terminal isoforms present in diffuse plaques and CVA of the aged dog and polar bear are similar to those found in the aged human brain. The absence of neuritic plaques in the aged dog and polar bear was not accounted for by differences in the types of Aβ N-terminal isoforms in diffuse plaques, as all examined species revealed the same isoforms. A lower abundance of extracellular N-terminal Aβ in the gray matter and the shorter lifespan of these species may partially explain their lack of neuritic plaques. The data suggest that each of the examined isoforms is associated with distinct patterns of deposition. Aβ17-x (the potentially nonamyloidogenic p3 fragment) was typically found in diffuse deposits and absent in neuritic plaques. AβN3(pE) (which is resistant to degradation) was most abundant in AD brain. A critical mass of this particular isoform may be necessary for the formation of neuritic deposits. The ratio of AβN3(pE) vs AβN17(L) is greater in the human brain than in the aged dog or polar bear. The polar bear exhibited similar amounts of p3 and less AβN3(pE) than nondemented human, while the canine demonstrated extremely low values of each p3 and AβN3(pE). Nondemented humans had substantially lower amounts of AβN3(pE) and p3 when contrasted with results in AD brain. AβN1(rD) was absent in AD neuritic plaques, but was present in control brain neuritic deposits of those affected by atherosclerotic and vascular hypertensive changes. In addition, AβN1(rD) was found in the CVA of individuals affected by both AD and atherosclerotic/vascular hypertensive changes, though this isoform was absent in the CVA of those solely affected by AD. The results provide additional evidence that parenchymal deposits in the aged dog and polar bear resemble relatively early stages of Aβ deposition in the human brain, whereas the CVA deposits in the beagle are similar to human CVA. The present study complements previous investigations that have addressed C-terminal heterogeneity of Aβ deposits in diffuse vs neuritic deposits and cerebrovascular amyloid. In conclusion, the data illustrate that distinct Aβ C- and N-terminal isoforms are associated with diffuse plaques, neuritic plaques, and CVA deposits (Table 6).

ACKNOWLEDGMENTS

We thank Dr Daron Davis for neuropathologic diagnoses of the human cases. This study was supported by NIA grant P50 AG05144-13 (WRM and JWG) and an NIMH NRSA predoctoral fellowship F31 MH11650 (TLT).

REFERENCES

1. Hamill RW, Markesbery WR, McDaniel K, Coleman PD. Characterization of brain samples in studies of aging, Alzheimer's, and other neurodegenerative diseases. Neurobiol Aging 1993;14:539–45
2. Kuo YM, Emmerling MR, Vigo-Pelfrey C, et al. Water-soluble ABeta (N-40, N-42) oligomers in normal and Alzheimer disease brains. J Biol Chem 1996;271:4077–81
3. Pike CJ, Walencewicz AJ, Glabe CG, Cotman CW. In vitro aging of beta-amyloid protein causes peptide aggregation and neurotoxicity. Brain Res 1991;563:311–14
4. Pike CJ, Burdick D, Walencewicz AJ, Glabe CG, Cotman CW. Neurodegeneration induced by β-amyloid peptides *in vitro*: The role of peptide assembly state. J Neuroscience 1993;13:1676–87
5. Mattson MP, Tomaselli KJ, Rydel RE. Calcium-destabilizing and neurodegenerative effects of aggregated beta-amyloid peptide are attenuated by basic FGF. Brain Res 1993;621:35–49
6. Lorenzo A, Yankner BA. β-amyloid neurotoxicity requires fibril formation and is inhibited by Congo Red. Proc Natl Acad Sci USA 1994;91:12243–47
7. Yamaguchi H, Nakazato Y, Shoji M, Takatama M, Hirai S. Ultrastructure of diffuse plaques in senile dementia of the Alzheimer type: Comparison with primitive plaques. Acta Neuropathologica 1991;82:13–20
8. Davies CA, Mann DM. Is the "preamyloid" of diffuse plaque in Alzheimer's disease really nonfibrillar? Amer J Pathol 1993;143:1594–1605
9. Selkoe DJ, Beli DS, Podlisny MB, Price DL, Cork LC. Conservation of brain amyloid proteins in aged mammals and humans with Alzheimer's disease. Science 1987;235:873–77
10. Cork LC, Masters C, Beyreuther K, Price DL. Development of senile plaques. Relationships of neuronal abnormalities and amyloid deposits. Amer J Pathol 1990;137:1383–92
11. Martin LJ, Sisodia SS, Koo EH, et al. Amyloid precursor protein in aged nonhuman primates. PNAS (USA) 1991;88:1461–65
12. Robakis NK, Pangalos MN. Involvement of amyloid as a central step in the development of Alzheimer's disease. Neurobiol Aging 1994;15:S127–S129
13. Tagliavini F, Ghiso J, Timmers WF, Giaccone G, Bugiani O, Frangione B. Coexistence of Alzheimer's amyloid precursor protein and amyloid protein in cerebral vessel walls. Lab Invest 1990;62:761–67
14. Johnstone EM, Chaney MO, Norris FH, Pascual R, Little SP. Conservation of the sequence of the Alzheimer's disease amyloid peptide in dog, polar bear, and five other mammals by cross-species polymerase chain reaction analysis. Brain Res Mol Brain Res 1991;10:299–305
15. Wisniewski T, Lalowski M, Bobik M, Russell M, Strosznajder J, Frangione B. Amyloid β1-42 deposits do not lead to Alzheimer's neuritic plaques in aged dogs. Biochem J 1996;313:575–80

16. Cummings BJ, Sato T, Head E, et al. Diffuse plaques contain C-terminal Aβ42 and not Aβ40: Evidence from cats and dogs. Neurobiol Aging 1996;17:653–59
17. Tekirian TL, Cole GM, Russell MJ, et al. Carboxy terminal of β-amyloid deposits in aged human, canine, and polar bear brains. Neurobiology of Aging 1996;17:249–57
18. Walker LC, Masters C, Beyreuther K, Price DL. Amyloid in the brains of aged squirrel monkeys. Acta Neuropathologica 1990;80: 381–87
19. Heilbroner PL, Kemper TL. The cytoarchitectonic distribution of senile plaques in three aged monkeys. Acta Neuropathol 1990;81: 60–65
20. Martin LJ, Pardo CA, Cork LC, Price DL. Synaptic pathology and glial responses to neuronal injury precede the formation of senile plaques and amyloid deposits in the aged cerebral cortex. Amer J Pathol 1994;145:1358–81
21. Bons N, Mestre N, Ritchie K, Petter A, Podlisny M, Selkoe D. Identification of amyloid beta protein in the brain of the small, short-lived Lemurian primate Microcebus murinus. Neurobiol Aging 1994;15:215–20
22. Geddes JW, Anderson KJ, Cotman CW. Senile plaques as aberrant sprout-stimulating structures. Exp Neurol 1986;94:767–76
23. Crain BJ, Burger PC. The laminar distribution of neuritic plaques in the fascia dentata of patients with Alzheimer's disease. Acta Neuropathol (Berl) 1988;76:87–93
24. Games D, Adams D, Alessandrini R, et al. Alzheimer-type neuropathology in transgenic mice overexpressing V717F β-amyloid precursor protein. Nature 1995;373:523–52
25. Checler F. Processing of the β-amyloid precursor protein and its regulation in Alzheimer's disease. J. Neurochem 1995;65:1431–43
26. Roher AE, Lowenson JD, Clarke S, et al. Structural alterations in the peptide backbone of beta-amyloid core protein may account for its deposition and stability in Alzheimer's disease. J Biol Chem 1993;268:3072–83
27. Mori H, Takio K, Ogawara M, Selkoe DJ. Mass spectrometry of purified amyloid β protein in Alzheimer's disease. J Biol Chem 1992;267:17082–86
28. Kim J, Kim K. The use of FAB mass spectrometry and pyroglutamate aminopeptidase digestion for the structure determination of pyroglutamate in modified peptides. Biochem Mol Biol Internat 1995;35:803–11
29. Barrow CJ, Zagorski MG. Solution structures of β peptide and its constituent fragments: relation to amyloid deposition. Science 1991; 253:179–82
30. Burdick D, Soreghan B, Kwon M, et al. Assembly and aggregation properties of synthetic Alzheimer's A4/β amyloid peptide analogs. J Biol Chem 1992;267:546–54
31. Jarrett JT, Berger EP, Lansbury PT. The carboxy terminus of the β-amyloid protein is critical for the seeding of amyloid formation: Implications for the pathogenesis of Alzheimer's disease. Biochemistry 1993;32:4693–97
32. Iwatsubo T, Odaka A, Suzuki N, Mizusawa H, Nukina N, Ihara Y. Visualization of A beta 42(43) and A beta 40 in senile plaques with end-specific A beta monoclonals: Evidence that an initially deposited species is A beta 42(43). Neuron 1994;13:45–53
33. Pike CJ, Overmann MJ, Cotman CW. Amino-terminal deletions enhance aggregation of beta-amyloid peptides *in vitro*. J Biol Chem 1995;270:23895–98
34. Saido TC, Iwatsubo T, Mann DMA, Shimada H, Ihara Y, Kawashima S. Dominant and differential deposition of distinct β-amyloid peptide species, AβN3(pE), in senile plaques. Neuron 1995;14: 457–66
35. Gowing E, Roher AE, Woods AS, et al. Chemical characterization of A beta 17-42 peptide, a component of diffuse amyloid deposits of Alzheimer disease. J Biol Chem 1994;269:10987–90
36. Mak K, Yang F, Vinters HV, Frautschy SA, Cole GM. Polyclonals to β-amyloid(1-42) identify most plaque and vascular deposits in Alzheimer cortex, but not striatum. Brain Res 1994;667:138–42
37. Yang F, Mak K, Vinters HV, Frautschy SA, Cole GM. Monoclonal antibody to the C-terminus of β-amyloid. Neuroreport 1994;5: 2117–20
38. Iwatsubo T, Saido TC, Mann DMA, Lee VM-Y, Trojanowski JQ. Full-length amyloid β(1-42(43) and amino terminally modified and truncated amyloid β42(43) deposit in diffuse plaques. Amer J Pathol 1996;149:1823–30
39. Higgins LS, Murphy Jr. GM, Forno LS, Catalano R, Cordell B. p3 β-Amyloid peptide has a unique and potentially pathogenic immunohistochemical profile in Alzheimer's disease brain. Amer J Pathol 1996;149:585–96
40. Lalowski M, Golabek A, LeMere CA, et al. The "nonamyloidogenic" p3 fragment (Amyloid β17-42) is a major constituent of Down's Syndrome cerebellar preamyloid. J Biol Chem 1996;271: 33623–31
41. Kida E, Wisniewski KE, Wisniewski HM. Early amyloid-β deposits show different immunoreactivity to the amino- and carboxy-terminal regions of β-peptide in Alzheimer's disease and Down's syndrome brain. Neurosci Lett 1995;193:105–8
42. Lemere CA, Blustajn JK, Yamaguchi H, Wisniewski T, Saido TC, Selkoe DJ. Sequence of deposition of heterogeneous amyloid β-peptides and APOE in Down Syndrome: Implications for initial events in amyloid plaque formation. Neurobiology of Disease 1996; 3:16–32
43. Russo C, Saido TC, DeBusk LM, Tabaton M, Gambetti P, Teller JK. Heterogeneity of water-soluble amyloid beta-peptide in Alzheimer's disease and Down's syndrome brains. FEBS Lett 1997; 409:411–16
44. Younkin SG. Evidence that Aβ42 is the real culprit in Alzheimer's disease. Ann Neurol 1995;37:287–88
45. McKhann G, Drachman D, Folstein M, Katzman R, Price D, Stadlan EM. Clinical diagnosis of Alzheimer's disease: Report of the NINCDS-ADRDA Work Group under the auspices of Department of Health and Human Services Task Force on Alzheimer's Disease. Neurology 1984;34:939–44
46. Khatchaturian ZS. Diagnosis of Alzheimer's disease. Arch Neurol 1985;42:1097–1104
47. Mirra SS, Heyman A, McKeel D, et al. The Consortium to Establish a Registry for Alzheimer's disease (CERAD) Part II. Standardization of the neuropathologic assessment of Alzheimer's disease. Neurology 1991;41:479–86
48. Kitomoto T, Ogomori K, Tateishi J, Prusiner SB. Formic acid pretreatment enhances immunostaining of cerebral and systemic amyloids. Lab Invest 1987;57:230–36
49. Smitt PA, Troost D, Louwerse ES, de Jong JM, van Kessel DT, de Leeuw MA. Temporal lobe pathology in amyotrophic lateral sclerosis. Do amyotrophic lateral sclerosis and Alzheimer's disese share a common etiological factor? Clin Neuropathol 1993;12:88–91
50. Saido TC, Yamao-Harigaya W, Iwatsubo T, Kawashima S. Amino- and carboxyl-terminal heterogeneity of β-amyloid peptides deposited in human brain. Neuroscience Letters 1996;215:173–76
51. Yamamoto T, Hirano A. A comparative study of modified Bielschowsky, Bodian, and Thioflavin S stains on Alzheimer's neurofibrillary tangles. Neuropathol Appl Neurobiol 1986;12:3–9
52. Wolman M, Bubis JJ. The cause of the green polarization color of amyloid stained with Congo Red. Histochemie 1965;4:351–56
53. Yamazaki T, Yamaguchi H, Okamoto K, Hirai S. Ultrastructural localization of argyrophilic substances in diffuse plaques of Alzheimer-type dementia demonstrated by methenamine silver staining. Acta Neuropathol 1991;81:540–45
54. Yamaguchi H, Hirai S, Morimatsu M, Shoji M, Harigaya Y. Diffuse type of senile plaques in the brains of Alzheimer's-type dementia. Acta Neuropathol 1988;77:113–19

55. Defigueiredo RJ, Cummings BJ, Mundkur PY, Cotman CW. Color image analysis in neuroanatomical research: Application to senile plaque subtype quantification in Alzheimer's disease. Neurobiol Aging 1995;16:211–23
56. Geddes JW, Tekirian TL, Soultanian NS, Ashford JW, Davis DG, Markesbery WR. Comparison of neuropathologic criteria for the diagnosis of Alzheimer's disease. Neurobiology of Aging 1997. Forthcoming.
57. Barrow CJ, Yasuda A, Kenny PTM, Zagorski MG. Solution conformations and aggregational properties of synthetic amyloid β-peptides of Alzheimer's disease. J Mol Biol 1992;225:1075–93
58. Dickson DW. The pathogenesis of senile plaques. J Neuropathol Exp Neurol 1997;56:321–39
59. Mann DMA. The pathological association between Down syndrome and Alzheimer's disease. Mech Ageing Dev 1988;43:99–136
60. Masliah E, Sisk A, Mallory M, Mucke L, Schenk D, Games D. Comparison of neurodegenerative pathology in transgenic mice overexpressing V717F β-amyloid precursor protein and Alzheimer's disease. J. Neurosci 1996;16:5795–5811
61. Games D, Carr T, Guido T, et al. Progression of Alzheimer-type neuropathology in PDAPP 717 V–>F transgenic mice. Soc Neurosci Abstr 1995;21:258
62. McDonald JK, Barret AJ. Mammalian proteases. London: Academic Press, 1986
63. Naslund J, Jensen M, Tjemburg LO, Thyburg J, Terenius L, Nordstedt C. The metabolic pathway generating p3, an Aβ-peptide fragment, is probably non-amyloidogenic. Biochem Biophys Res Commun 1994;204:780–87
64. Velazquez P, Cribbs DH, Poulos TL, Tenner AJ. Aspartate residue 7 in amyloid beta-protein is critical for classical complement pathway activation: Implications for Alzheimer's disease pathogenesis. Nat Med 1997;3:77–79
65. Shapira R, Austin GE, Mirra SS. Neuritic plaque amyloid in Alzheimer's disease is highly racemized. J Neurochem 1988;50:69–74
66. Bada L. In vivo racemization in mammalian proteins. In: Wold F, Moldave K, eds. Methods in enzymology. 1984:99–115
67. Tomiyama T, Asano S, Furiya Y, Shirasawa T, Endo N, Mori H. Racemization of Asp^{23} residue affects the aggregation properties of Alzheimer amyloid β protein analogues. J. Biol Chem 1994;269: 10205–8
68. Sparks DL, Scheff SW, Liu H, et al. Increased density of senile plaques (SP), but not neurofibrillary tangles (NFT), in nondemented individuals with the apolipoprotein E4 allele: Comparison to confirmed Alzheimer's disease patients. J Neurological Sci 1996;138: 97–104
69. Haass C, Hung AY, Schlossmacher MG, Teplow DB, Selkoe DJ. Beta-amyloid peptide and a 3-kDa fragment are derived by distinct cellular mechanisms. J Biol Chem 1993;268:3021–24
70. Busciglio J, Gabuzda D, Matsudaira P, Yankner B. Generation of β-amyloid in the secretory pathway in neuronal and nonneuronal cells. PNAS USA 1993;90:2092–96
71. Bodovitz S, Klein WL. Cholesterol modulates alpha-secretase cleavage of amyloid precursor protein. J Biol Chem 1996;23:4436–40
72. Wild-Bode C, Yamazaki T, Capell A, et al. Intracellular generation and accumulation of amyloid β-peptide terminating at amino acid 42. J Biol Chem 1997;272:16085–88
73. Turner RS, Suzuki N, Chyung AS, Younkin SG, Lee VM. Amyloids beta 40 and beta 42 are generated intracellularly in cultured human neurons and their secretion increases with maturation. J Biol Chem 1996;271:8966–70
74. Klafki H, Abramowski D, Swoboda R, Paganetti PA, Staufenbiel M. The carboxyl termini of beta-amyloid peptides 1-40 and 1-42 are generated by distinct gamma-secretase activities. J Biol Chem 1996;271:28655–59
75. LeBlanc AC, Papadopoulos M, Belair C, et al. Processing of amyloid precursor protein in human primary neuron and astrocyte cultures. J Neurochem 1997;68:1183–90
76. Haass C, Koo EH, Teplow DB, Selkoe DJ. Polarized secretion of beta-amyloid precursor protein and amyloid beta-peptide in MDCK cells. PNAS 1994;91(4):1564–68
77. Podlisny MB, Ostaszewski BL, Squazzo SL, et al. Aggregation of secreted amyloid β-protein into sodium dodecyl sulfate-stable oligomers in cell culture. J Biol Chem 1995;270:9564–70
78. Haass C, Hung AY, Selkoe DJ, Teplow DB. Mutations associated with a locus for Familial Alzheimer's disease result in alternative processing of amyloid β-precursor protein. J Biol Chem 1994;269: 17741–48

Received February 27, 1997
Revision received September 4, 1997
Accepted September 26, 1997